HGS based CWNN- Hunger Game Search based Convolutional Wavelet Neural Network for Climate Change Detection

Aiswarya Jeevan
Department of Electronics and Communication Engineering
Noorul Islam Centre For Higher Education
Tamil Nadu, India
Aiswarya.Jeevan.321@outlook.com

S Amala Shanthi
Department of Electronics and Communication Engineering
Noorul Islam Centre For Higher Education
Tamil Nadu, India
Amala.Shanthi.321@outlook.com

2024 1st International Conference on Trends in Engineering Systems and Technologies (ICTEST) | 979-8-3503-0779-5/24/$31.00 ©2024 IEEE | DOI: 10.1109/ICTEST60614.2024.10576147

***Abstract*— Climate change is a critical issue that requires effective monitoring and timely intervention. Remote sensing techniques and machine learning algorithms have shown potential for detecting climate change, and several models have been proposed in recent years. The research contributes towards enhancing climate change detection capabilities, which are vital for addressing environmental challenges and understanding the impacts of climate change. This study introduces a new strategy for climate change detection according to Hunger Game Search (HGS) algorithm and Convolutional Wavelet Neural Network (CWNN), named HGS-based CWNN. CWNN algorithm has been shown to perform well in a variety of classification tasks, achieving high levels of accuracy. Also, HGS algorithm is highly explorative, which means that it is capable of finding solutions in an efficient manner, and does not get stuck in local optima. Thus, training CWNN using HGS algorithm can improve the performance further. The method is evaluated on two benchmark datasets, and the findings display its effectiveness in detecting climate change patterns with higher accuracy rate of 0.976% and lower MSE rate of 0.023. In general, the evaluation found that the suggested model displayed superior performance compared to established models in terms of precision and mean squared error (MSE).**

Keywords*— *Climate change detection, Hunger Games Search, CWNN, accuracy

I. INTRODUCTION

Remote sensing satellite imagery is widely utilized for land cover change monitoring, aiding in addressing environmental challenges such as wildfires, droughts, climate change, and carbon budgets [5]. The crucial process of change detection involves identifying and extracting information from multiple observations, focusing on land use and cover changes, forest monitoring, ecosystem health evaluation, urban expansion research, resource management, and disaster damage assessment [11]. The advancements in satellite imaging technology, providing high-resolution images, have facilitated the acquisition of spatially rich data for change detection [12]. Despite these benefits, challenges persist in efficiently extracting and comprehending feature-rich data, minimizing interference from pseudo-changes, and enhancing accuracy in remote sensing change detection [1].

Remote sensing change detection, utilizing spectral information from remote sensing data, is a crucial technique for extracting information about alterations in land surface features [8]. Widely applied in areas such as land management, disaster assessment, urban expansion research, and resource management, this process addresses diverse challenges in identifying changing targets within remotely sensed time series marked by uneven spacing and the presence of trend, seasonal, and other components [3]. While traditional methods like BFAST, CCDC, STL, and DBEST focus on non-stationary time series, they often assume evenly spaced data and overlook experimental errors. In contrast, the increasing success of Machine Learning (ML) methods in fields like 3D scene understanding and natural language processing has fueled interest in the remote sensing community for Deep Learning (DL) methods. These DL techniques exhibit robust, human-like reasoning characteristics, capturing input image semantics effectively [5].

This paper introduces a novel approach, Hunger Game Search-Based Convolutional Wavelet Neural Network (HGS-CWNN), for change detection. The hybrid model, CWNN, combines convolutional neural networks (CNNs) and wavelet transforms to effectively handle intricate image features. The training process utilizes the Hunger Game Search (HGS) algorithm, a population-based search inspired by the survival of the fittest concept. The HGS-CWNN model employs convolutional and wavelet filters in multiple layers to extract and process diverse input image features, enhancing detection accuracy. Throughout training, the HGS algorithm optimizes weights and filters for improved performance on the dataset.

The primary objective of the study is as follows,

- To advance a deep learning trained with optimization algorithm, named Hunger Game Search- based Convolutional Wavelet Neural Network (HGS-based CWNN) for climate change detection.
- To estimate the efficiency of the presented model by means of metrics, such as error and accuracy.

The paper is organized as follows: Section II reviews previous change detection models, Section III details the proposed HGS-based CWNN approach, Section IV presents results and discussion, and Section V concludes the study.

II. RELATED WORKS

The literature survey highlights studies on change detection. Chen et al. [1] introduced a dual attentive fully convolutional Siamese network, effectively filtering irrelevant changes and improving recognition performance. Pal et al. [2] proposed a unique algorithm for pixel-level segmentation of multi-spectral very high-resolution images, employing variable-length multi-objective genetic clustering. This approach,

retaining variable-length properties in optimization, demonstrated effectiveness in large-scale change detection, outperforming state-of-the-art techniques in evaluations with Pleiades-HR 1B and Landsat 5 TM datasets.

Hou et al. [3] explored the HRTNet framework, incorporating a dynamic inception module for bi-temporal image learning. The triplet input network emphasized temporal variations, while a separate network preserved high-resolution image characteristics. The dynamic inception module enhanced feature expression, improving multi-scale information extraction. The framework demonstrated efficacy and robustness in detecting changes across three widely-used high-resolution image remote sensing datasets.

Peng et al. [4] introduced a CD technique, UNet++, utilizing an efficient encoder-decoder architecture for semantic segmentation. The improved UNet++ network concatenated pairs of images, allowing for fine-grained and global information integration. Fusion of change maps from various semantic levels resulted in precise spatial information. The method demonstrated reliability and efficiency on VHR satellite image datasets. Ghaderpour and Vujadinovic [5] proposed JUST, a method for detecting abrupt changes in time series data using ALLSSA and temporal segmentation. JUST performed well in detecting jumps, outperforming the BFAST method in identifying abrupt changes in the trend component of time series with various types, as demonstrated on simulated and real-world vegetation time series from southeastern Australia.

A. Challenges

Based on the difficulties identified with existing approaches mentioned earlier, the study gaps found are as follows: The DASNet [1] faced issues in handling small samples and challenging environments, and also failed to enhance the mobility and robustness in change detection. CWNN [1] has a complex architecture due to the convolutional layers and wavelet transforms, making them challenging to train and optimize. Additionally, the optimal choice of hyperparameters is difficult to determine, which can hinder performance. Likewise, the approach developed in [2] did not efficiently identify the automatic change detection concerns and also the method in [3] failed to explore the detection performance by utilizing a comparatively smaller quantity of training examples. In addition, the approach mentioned in [4] did not exploit the weakly supervised learning and sample generation approaches and did not examine the ability to create semantic connections for the modified regions.

III. METHODOLOGY

The study aims to develop a climate change detection strategy using remote sensing images. The schematic view of the proposed HGS-based CWNN model is depicted in Fig.1. Leveraging fully convolutional neural networks for efficient parallel processing of large input images, the model achieves faster performance compared to other methods. The HGS algorithm [7] is employed for training the CWNN, enhancing accuracy through optimization. The study demonstrates improved climate change detection performance using remote sensing images.

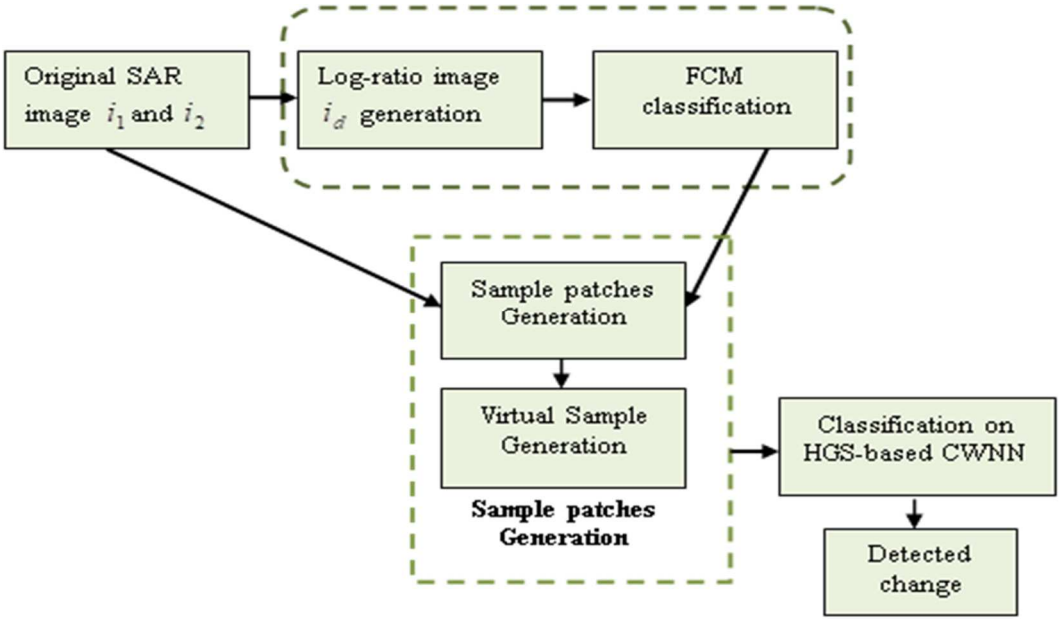

Fig.1. Schematic diagram of the presented HGS-based CWNN method for climate change detection

A. Pre-classification

To generate a difference image i_d , the log-ratio operator is implemented, followed by the application of the FCM algorithm for the classification of the difference image into three different clusters. The long ratio image i_d is calculated using the formula$i_d = \left|log \frac{i_2}{i_1}\right|$. Prior to change analysis, the SAR image's linear scale is transformed into a logarithmic scale through the use of the log-ratio operator. This transformation enables conversion of multiplicative noise to additive noise after calculating i_d. The calculation of the log-ratio image is carried out by using a formula. Subsequently, pixels are classified into three categories – changed Ω_c, unchanged Ω_u , and intermediate Ω_I - through a hierarchical FCM algorithm applied to the log-ratio image. Pixels belonging to the changed Ω_c and unchanged classes Ω_u are selected as training samples. Further classification of pixels in the intermediate class Ω_I is achieved through CWNN.

Using FCM in the HGS-based CWNN approach is relevant for noise reduction, simplifying analysis, selecting training samples, handling intermediate changes, and ultimately improving the overall performance of the climate change detection model

B. Image patch generation

Here, image patches are created around each pixel in the SAR images. The patches with a high likelihood of being unchanged or changed are used as training samples, and virtual samples are also created. The patches concentrated to pixels belongs to *c* and *u*, denote changed and, unchanged classes that are derived from the original images. A patch $p_k{}^{I_1}$ concentrated at pixel *k* in image I_1 is represented by $p_k{}^{I_2}$, and its corresponding patch in image I_2 . These patches have a size of *w x w*. To concatenate the two patches, a new image patch p_k is created with a size of *2w x w*. The number of pixels affiliated with the unchanged and changed classes is represented by N, and from these classes, sample images $\{p_k\}, k = 1,2, \dots, N$ are obtained. The features of these sample images are then extracted and trained using CWNN. However, tuning the weights in CWNN is a complicated task, as there are many weights involved in the process. Since there are many weights in CWNN, inappropriate weights aid to detect changes. To overcome this problem, virtual samples are generated to enrich the training examples. A virtual sample p_k can be created using two provided examples of the same class with appropriate ratios. Although the number of available samples in SAR image change detection is limited, the method proposes the use of virtual samples to enhance the training process.

$$p_k{}' = \alpha p_x + (1 - \alpha) p_y + \beta \qquad (1)$$

The proposed method for generating virtual samples involves randomly choosing two training samples p_k and p_y from the same class and combining them with a uniformly distributed random value, denoted as α, and a random Gaussian noise β, with a mean value of 0 and a variance value of 0.001. This approach is similar to the method used in hyperspectral image classification [18], where virtual sample $p_k{}'$ was shown to improve classification performance when training data is limited. Since the virtual sample created using two examples from the same class also belong to the same class, it is assigned the same label as the original training samples. N samples from $\{p_k\}, k = 1,2, \dots, N$ are then randomly selected, and combined with the virtual samples to form a larger training set for the CWNN, which is used to obtain optimal weights for classification.

C. Change Detection using HGS-based CWNN

1) CWNN

CWNN is designed to learn discriminative factors that distinguish changed information from multi-temporal Synthetic Aperture Radar (SAR) images. Similar to CNN, CWNN contains max-pooling layers convolutional layers, and fully connected layers, that capture fundamental visual characteristics like corners, endpoints, and oriented edges, at the beginning layer. Moreover, the intrinsic speckle noise in the images of SAR can negatively impact classification performance. While CNN uses max-pooling layers to reduce complexity and retain essential information, this approach can cause the loss of crucial structures, like corners, and edges that are important in SAR image classification. To address this issue, a new approach called CWNN [15] combines CNN with the DWT and its DT-CWT variation to lessen the impact of speckle noise. DT-CWT provides perfect reconstruction, limited redundancy, and superior directional selectivity, thereby facilitating effective decomposition of the previous layer to create eight components. These components include two low-frequency sub-bands LL1 and LL2 and six high-frequency sub-bands in orientations including ±15◦, ±45◦, and ±75◦ (represented by lh_1, lh_2, hl_1, hl_2 and hh_2). The pooling layer's output is determined by choosing the mean value from the two sub-bands with low frequencies, which preserves more critical structures and helps improve classification accuracy in SAR images.

Incorporating DT-CWT into CNN provides two significant benefits. Firstly, the low-frequency sub-bands maintain the input layer's structures according to defined rules, ensuring a more precise representation of the input. Secondly, the removal of high-frequency sub-bands through wavelet pooling aids in suppressing speckle noise. The approach utilizes the output of the preceding convolutional layer as input to the wavelet pooling layer, obtaining multiple sub-bands through DT-CWT, as outlined in Equation (2).

$$ll_1, ll_2, lh_1, lh_2, hl_1, hl_2, hh_1, hh_2 = f(y_1) \qquad (2)$$

where, the DT-CWT function (.) is used to generate eight components. The mean of the sub-bands with low frequencies is then utilized as the output value of the wavelet pooling layer. This is explained as in Equation (3).

$$ll_{mean} = \frac{1}{2}(ll_1 + ll_2) \qquad (3)$$

The output value of the wavelet pooling layer is denoted by ll_{mean} , and the structure of the CWNN is presented in Fig.2. The first and second convolutional layers are denoted as c_2 and c_4 , respectively, while the wavelet pooling layers are denoted as w_3 and w_5. The network consists of layers $\{i_1, c_2, w_3, c_4, f_6, o_7\}$, where serves as the input layer. The input image patches are first resized to 28×14. Layer c_2 is a convolutional layer with six 5×3 kernels, which creates six feature maps of size 24×12. The wavelet pooling layer is showed as w_3 and w_5, and it decomposes all the input feature maps with one-level DT-CWT. This layer manufactures six feature maps with a size of 12×6. Layer w_5 is a convolutional layer with 12 5×3 kernels, which produces 12 feature maps of size 8×4. A wavelet pooling layer follows, and it generates 12 feature maps with a size of 4×2. Layer f_6 is a fully connected layer consisting of 96 units, while layer o_7 serves as the output layer, consisting of two units that represent the unchanged and changed classes, respectively. The integration of CWT into CNN in CWNN effectively mitigates speckle noise by applying DT-CWT, resulting in a refined SAR image representation and improved accuracy in change detection

2) Training using HGS Algorithm

The HGS algorithm trains CWNN by iteratively sampling from a hierarchical Gaussian distribution, adjusting network weights for effective learning from large datasets. Utilizing a hierarchical distribution facilitates efficient weight adjustments at multiple network levels, capturing complex input-output relationships. The training set combines real and virtual samples into a unified set, promoting diversity and

balance in CWNN learning. After training, image patches from Ω_l are categorized into unchanged or changed classes, and the pre-classification outcome is merged with CWNN findings to generate the final change map [21]. This approach enhances CWNN's learning experience, leading to improved generalization and performance in change detection tasks.

IV. RESULTS AND DISCUSSION

The proposed algorithm was evaluated using the PYTHON tool and the "Change Detection Dataset (CDD) [6]." Performance assessment involved comparing two parameters, MSE and accuracy. Traditional approaches, including NSGA-II [2], HRTNet [3], and JUST [5], served as benchmarks for performance comparison.

A. Change Detection Dataset (CDD)

The Change Detection Dataset (CDD) is a widely-used benchmark in remote sensing, offering high-resolution satellite images captured at different times, showcasing diverse land use and land cover changes. It includes temporal and spectral bands, along with binary reference maps indicating change presence or absence. CDD serves as a valuable resource for testing new models and algorithms in remote sensing applications.

B. Image Results

The results, depicted in Fig.2, showcase sample images 1 and 2. Images (a) and (b) represent input images 1 and its alternative view, while (c) demonstrates change detection for image 1 with its ground truth in (d). Image 2 and its alternate view are shown in (e) and (f). The change detection output for image 2 by the proposed HGS-based CWNN is illustrated in (g), and its ground truth is in (h). This analysis accurately identifies differences between input images, offering valuable insights into the potency of the presented technique for change detection.

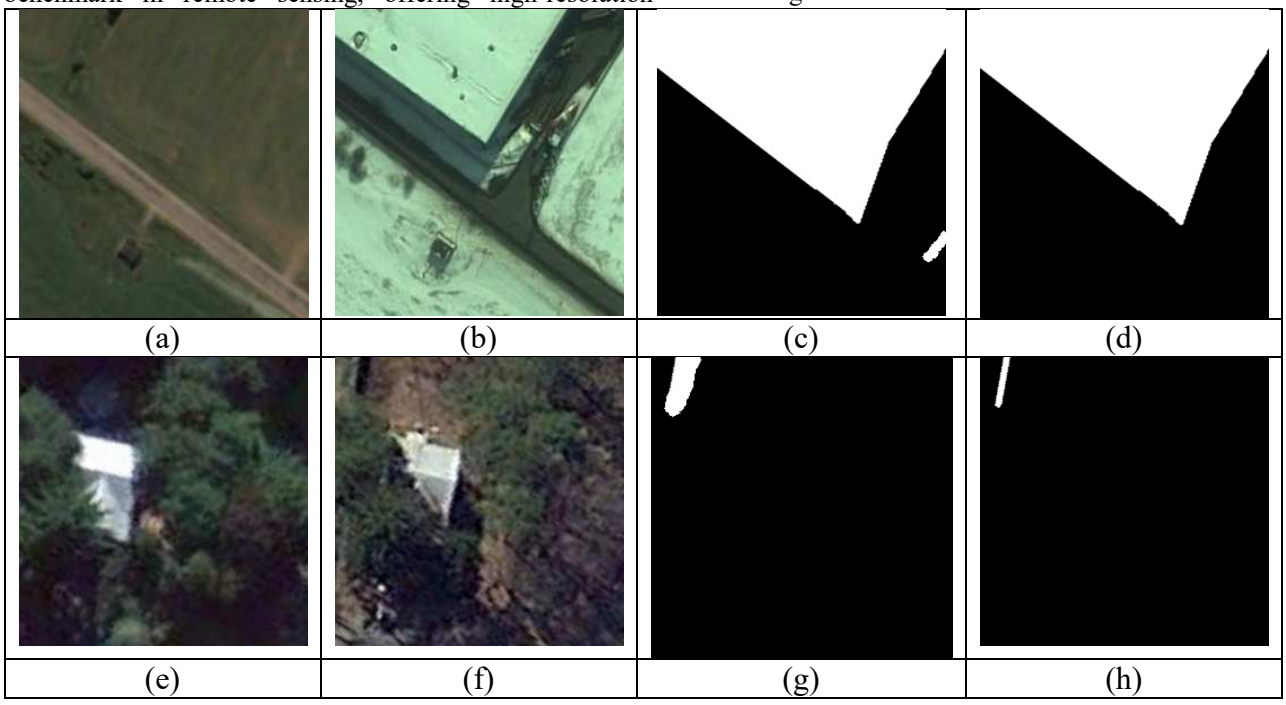

Fig.2. (a), Input image 1, (b) view of image 1 in alternate angle, (c) detected change in image 1, (d) ground truth of image 1, (e), Input image 2, (f) view of image 2 in alternate angle, (g) detected change in image 2, (h) ground truth of image 2.

C. Performance Analysis

In this section, the performance of the HGS-based CWNN model is evaluated for two images, denoted as image 1 and 2. Fig.3 presents the accuracy and MSE results for both images. For image 1, the HGS-based CWNN achieved an accuracy of 0.923 at iteration 20 with a block size of 4, increasing to 0.9696 at iteration 80 with a block size of 10 Fig.3 (a). Similarly, for image 2, the accuracy improved from 0.9507 at iteration 60 with block size of 6 to 0.9764 at iteration 100 with block size 10 in Fig.3 (b). Regarding MSE, for image 1, it reduced from 0.0606 at iteration 60 with block size of 4 to 0.0303 at iteration 80 with block size of 10 Fig.3 (c). For image 2, the MSE decreased from 0.0723 at iteration 20 with block size of 4 to 0.0235 at iteration 100 with block size of 10 Fig.3 (d).

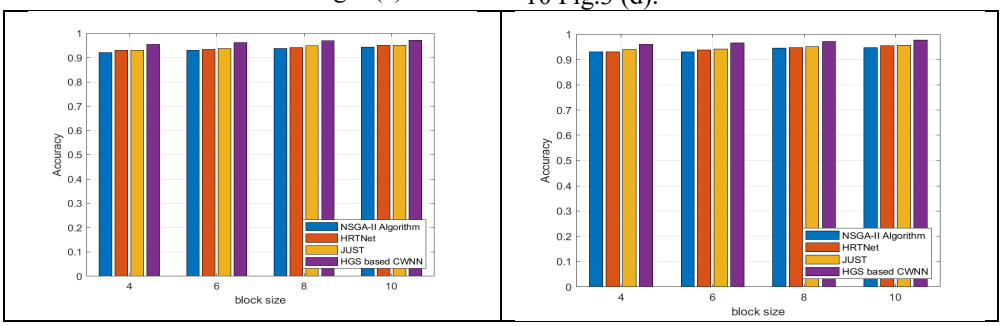

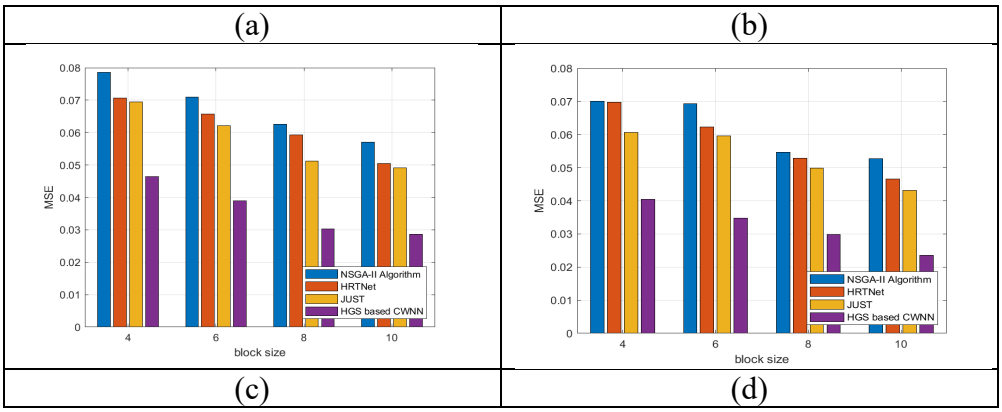

Fig.3. Performance analysis of Proposed HGS-based CWNN model (a) accuracy of image 1 (b) accuracy of image 2 (c) MSE of image 1 (d) MSE of image 2.

D. Comparative Analysis

Fig. 4 illustrates the accuracy and MSE comparisons between the HGS-based CWNN and other models for image 1 and image 2. In Fig. 4 (a), the HGS-based CWNN achieved an accuracy of 0.953 for block size of 4, outperforming HRTNet (0.9293) and JUST (0.9305). Fig. 4 (b) shows an accuracy of 0.9702 for HGS-based CWNN for block size of 8 in image 2, while NSGA-II Algorithm and HRTNet achieved accuracies of 0.945 and 0.9470, respectively. MSE comparisons in Fig. 4 (c) reveal an MSE of 0.0303 for HGS-based CWNN for block size of 8 in image 1, surpassing HRTNet (0.0592) and JUST (0.0511). In Fig. 4d, for image 2, HGS-based CWNN achieved an MSE of 0.02357 for block size of 10, outperforming NSGA-II Algorithm (0.0527) and JUST (0.0431)

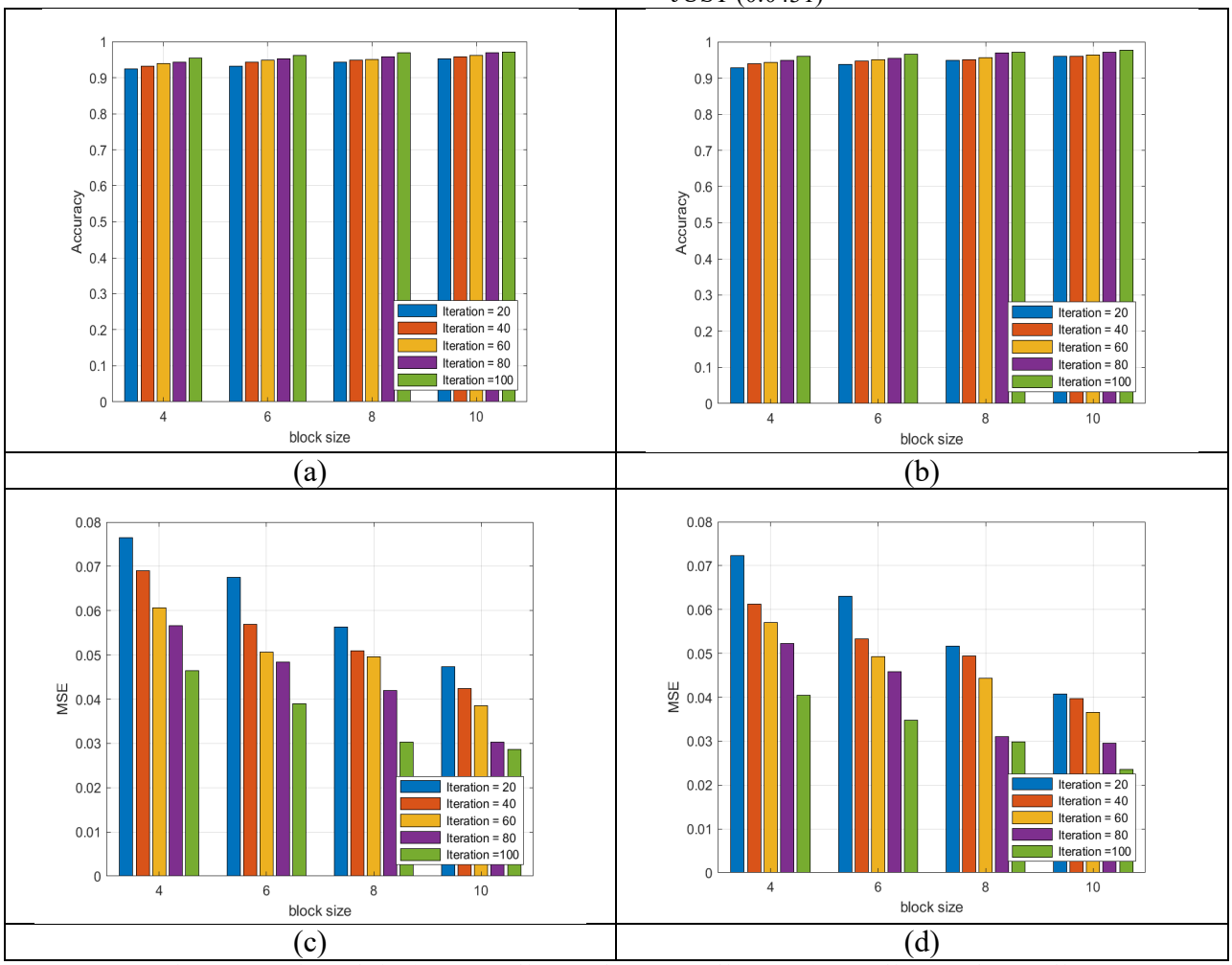

Fig.4. Comparative analysis (a) accuracy of image 1 (b) accuracy of image 2 (c) MSE of image 1 (d) MSE of image 2.

Table I summarizes the comparative analysis of the HGS-based CWNN with conventional models (NSGA-II Algorithm, HRTNet, and JUST) in terms of accuracy and MSE. The proposed model demonstrated a 2.98% higher accuracy than NSGA-II Algorithm for image 1, and a 42.85% lower MSE than JUST for the same image. For image 2, the proposed model showed a 2.35% higher accuracy compared to HRTNet. The overall assessment suggests that the HGS-based CWNN outperforms traditional models in terms of both accuracy and MSE.

TABLE.I COMPARATIVE DISCUSSION OF PROPOSED HGS-BASED CWNN WITH OTHER CONVENTIONAL MODELS

Metrics	NSGA-II Algorithm	HRTNet	JUST	HGS-based CWNN
Accuracy	0.947	0.953	0.956	**0.976**
MSE	0.052	0.046	0.043	**0.023**

V. CONCLUSION

The research contributes towards enhancing climate change detection capabilities, which are vital for addressing environmental challenges and understanding the impacts of climate change. The proposed HGS-based CWNN approach for climate change detection shows promising results and improved performance compared to existing techniques. The use of the Hunger Game Search algorithm and the convolutional wavelet neural network greatly enhances the accuracy of climate change detection. The results elucidate the proposed HGS based CWNN shows increased in accuracy and lesser error. According to the results of the experiment, the proposed HGS based CWNN model reached the highest level of accuracy of 0.976% and MSE of 0.023. The overall analysis of the experiment indicates that the proposed model showed improved outcomes in regards to accuracy and MSE when compared to conventional models. The future scope of the study can be extended to include more sources of climate data and enhance the analysis of climate change over longer periods.

REFERENCES

[1] J. Chen, Z. Yuan, J. Peng, L. Chen, H. Huang, J. Zhu, Y. Liu, and H. Li, "DASNet: Dual attentive fully convolutional Siamese networks for change detection in high-resolution satellite images," IEEE J. Sel. Topics Appl. Earth Observ. Remote Sens., vol. 14, pp. 1194-1206, 2020.

[2] R. Pal, S. Mukhopadhyay, D. Chakraborty, and P. N. Suganthan, "Very high-resolution satellite image segmentation using variable-length multi-objective genetic clustering for multi-class change detection," J. King Saud Univ.-Comput. Inf. Sci., vol. 34, no. 10, pp. 9964-9976, 2022.

[3] X. Hou, Y. Bai, Y. Li, C. Shang, and Q. Shen, "High-resolution triplet network with dynamic multiscale feature for change detection on satellite images," ISPRS J. Photogramm. Remote Sens., vol. 177, pp. 103-115, 2021.

[4] D. Peng, Y. Zhang, and H. Guan, "End-to-end change detection for high resolution satellite images using improved UNet++," Remote Sensing, vol. 11, no. 11, pp. 1382, 2019.

[5] E. Ghaderpour and T. Vujadinovic, "Change detection within remotely sensed satellite image time series via spectral analysis," Remote Sensing, vol. 12, no. 23, pp. 4001, 2020.

[6] Change detection dataset (CDD), https://github.com/lehaifeng/DASNet, accessed on July 2023.

[7] Y. Yang, H. Chen, A. A. Heidari, and A. H. Gandomi, "Hunger games search: Visions, conception, implementation, deep analysis, perspectives, and towards performance shifts," Expert Syst. Appl., vol. 177, pp. 114864, 2021.

[8] R. J. Radke, S. Andra, O. Al-Kofahi, and B. Roysam, "Image change detection algorithms: a systematic survey," IEEE Trans. Image Process., vol. 14, no. 3, pp. 294-307, 2005.

[9] N. Goyette, P.-M. Jodoin, F. Porikli, J. Konrad, and P. Ishwar, "Changedetection. net: A new change detection benchmark dataset," in 2012 IEEE Comput. Soc. Conf. Comput. Vis. Pattern Recognit. Workshops, pp. 1-8, IEEE, 2012.

[10] J. R. G. Townshend, C. O. Justice, C. Gurney, and J. McManus, "The impact of misregistration on change detection," IEEE Trans. Geosci. Remote Sens., vol. 30, no. 5, pp. 1054-1060, 1992.

[11] M. T. Yilmaz, E. R. Hunt Jr, and T. J. Jackson, "Remote sensing of vegetation water content from equivalent water thickness using satellite imagery," Remote Sens. Environ., vol. 112, no. 5, pp. 2514-2522, 2008.

[12] S. L. Ozesmi and M. E. Bauer, "Satellite remote sensing of wetlands," Wetlands Ecol. Manage., vol. 10, pp. 381-402, 2002.

[13] S. Dhingra and D. Kumar, "A review of remotely sensed satellite image classification," Int. J. Electr. Comput. Eng., vol. 9, no. 3, pp. 1720, 2019.

[14] D. R. Sowmya, P. D. Shenoy, and K. R. Venugopal, "Remote sensing satellite image processing techniques for image classification: a comprehensive survey," Int. J. Comput. Appl., vol. 161, no. 11, pp. 24-37, 2017.

[15] P. M. Dare, "Shadow analysis in high-resolution satellite imagery of urban areas," Photogramm. Eng. Remote Sens., vol. 71, no. 2, pp. 169-177, 2005.

[16] F. Gao, X. Wang, Y. Gao, J. Dong, and S. Wang, "Sea ice change detection in SAR images based on convolutional-wavelet neural networks," IEEE Geosci. Remote Sens. Lett., vol. 16, no. 8, pp. 1240-1244, 2019.

[17] G. Xian, C. Homer, and J. Fry, "Updating the 2001 National Land Cover Database land cover classification to 2006 by using Landsat imagery change detection methods," Remote Sens. Environ., vol. 113, no. 6, pp. 1133-1147, 2009.

[18] J. Liu, M. Gong, K. Qin, and P. Zhang, "A deep convolutional coupling network for change detection based on heterogeneous optical and radar images," IEEE Trans. Neural Netw. Learn. Syst., vol. 29, no. 3, pp. 545-559, 2016.

[19] Y. Zhan, K. Fu, M. Yan, X. Sun, H. Wang, and X. Qiu, "Change detection based on deep siamese convolutional network for optical aerial images," IEEE Geosci. Remote Sens. Lett., vol. 14, no. 10, pp. 1845-1849, 2017.

[20] J. Tang, L. Jin, Z. Li, and S. Gao, "RGB-D object recognition via incorporating latent data structure and prior knowledge," IEEE Trans. Multimedia, vol. 17, no. 11, pp. 1899-1908, 2015.